

## FLOW CHARACTERISTICS AND VISUALIZATION OF RECTANGULAR SLOT AIR JET IMPINGEMENT AGAINST FLAT SURFACES

**\*Akhil S.<sup>1</sup>, Varun T.<sup>2</sup>, Raghavendra K.<sup>3</sup>, Nivedita D.<sup>4</sup>**

<sup>1</sup>Assistant Professor, RajaRajeswari College of Engineering, Bengaluru, Karnataka, India

<sup>2</sup>Formerly-Professor & Chairperson of Department of Mechanical Engineering, University Visvesvaraya College of Engineering, Dean Engineering faculty, Bangalore University, Bengaluru

Presently-Professor, Nitte Meenakshi Institute of Technology, Bengaluru, Karnataka, India

<sup>3</sup>P.G Student, University Visvesvaraya College of Engineering, Bengaluru, Karnataka, India

<sup>4</sup>Professor, University Visvesvaraya College of Engineering, Bengaluru, Karnataka, India

### **ABSTRACT**

Jet impingement near the mid-chord of the gas turbine blade is treated as a flat plate. Experimental and numerical investigations are carried out for a single slot air jet impinging on flat surface for two different rectangular slots of dimension (3mm x 65 mm) and (5mm x 65 mm). Experimentation is done to study the flow pattern topography on the flat target plate, with varying the flow rate from 20 LPM to 50 LPM by varying the nozzle to plate distance from 9 mm to 24 mm for slot jet of 3mm and varying the nozzle to plate distance from 10 mm to 30 mm for slot jet of 5mm. Lampblack flow visualization technique has been used for visualizing the flow pattern of impinging jets on the flat plate. The computational results have been compared with experimental by solving the set of governing equation have been solved for flowing fluid over the geometry. The Navier-Stokes equations are solved for steady flow turbulent cases. The flat plate problem has been modeled and meshed in Ansys 14.5 workbench and solved in Fluent. The numerical analysis is validated with experimental work, and it is found that the computational results are agreeing with experimental results with an error less than 15% indicating that the CFD analysis can be used reliably for visualizing the flow pattern for different configurations of single slot jet impingement. From current research study it is revealed that maximum shear zone width is influences in selection of neighboring jets besides the primary jet. For case considered for study the neighboring jets should be selected 15 mm away from the stagnation zone there by secondary heat transfer peaks can be achieved so that it enhances heat transfer in multi jet impingement cooling. This study gives clear idea how to choose multi slot jets side by side at correct distance from central stagnation zone. It also helps in avoiding abrasion of the surface particulates for mass transfer applications. Selection of efficient configuration of multi slot impingement arrangements offers efficient use of the fluid and for maintaining necessary cooling rate.

**KEYWORDS:** Flow visualization, Jet impingement, Rectangular slot, Flat plate, CFD analysis.

### **I. INTRODUCTION**

Jet impingement technique is used in wide variety of engineering applications where high rates of heat or mass transfer is needed. The impingement of an issuing jet onto a solid surface enhances local heat transfer rates during heating, cooling or drying the surfaces. The best example are heating or cooling of metal plates, drying of papers, textiles, and food stuffs, cooling of turbine blades and cooling of electronic components and de-icing of aircraft wings. The flow and heat transfer characteristics of such flows have been the subject of large number of theoretical and experimental studies. The jet impinging on flat surfaces is of great interest in most of industrial application. The impingement cooling heat transfer has been extensively studied from last many years. The impinging jet flow basically consists of a nozzle or nozzle array, a target surface and jet flow between these two objects. The flow component can be in confined or unconfined environment. The velocity and temperature profile, local and averaged heat transfer rates (Nusselt number) around or at surface have been main concern. The effective parameters on the resulting nonlinear flow, static pressure distribution and heat transfer are known to be nozzle geometry, jet orientation, jet Reynolds number, nozzle to surface spacing, jet to jet spacing and shape of the target surface. Jet impingement is used as an effective mechanism for achieving high localized transport rates. Single or multiple rows of jet are used to achieve this objective, the most commonly used geometries are axi-symmetric (circular orifice), slot (two dimensional) nozzles, rectangular and square (three dimensional) nozzles. In the present work, experimental and numerical investigation of a single slot jet impinging on flat surface is studied. Jet impingement near the mid-chord of the gas turbine blade is treated as a flat plate. Experimentation is done to study the flow pattern topography on the flat target plate, with varying the flow rate (Reynolds number) from 20 LPM to 50 LPM and varying H/w ratio for two different slots of 3mm and 5mm. Lampblack flow visualization on a target plate is done to study the flow pattern characteristics quantitatively. The visualization technique is used to verify the impinging procedure and used as basic information for studying the behavior of impinging jets.

Impinging jet contains simple geometry and simple in operation. But it contains extremely complex flow physics. The impinging involves three different regions.

1. Free jet flow region.
2. Stagnation flow region.
3. Wall jet flow region.

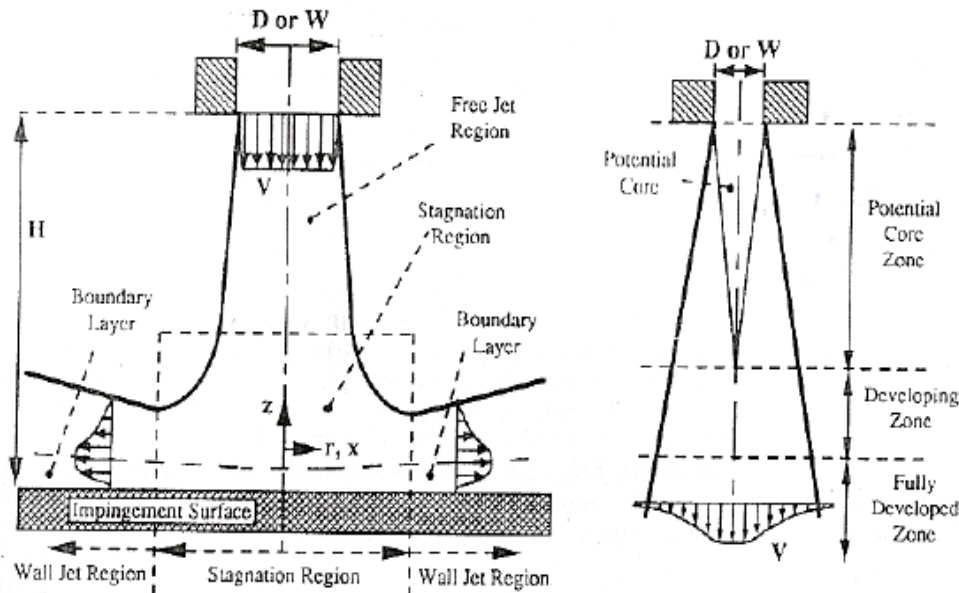


Figure.1: The flow regions of impinging jet [1]

These regions are shown in Figure.1. It indicate the normalized geometrical parameters D (Diameter of the jet), H (Height from jet to target plate), x (radial direction of the flow).The Reynolds number (Re) is defined by the velocity inlet from the jet. The vectors in this figure shows hypothetical velocity field for a true impinging jet, but it is not this much structured. This involves highly unsteady and several flow phenomena.

This includes instability, non-linear vortex interaction, transition, vortex break down and separation. Flow characteristics and wall heat transfer of conventional impinging jets depend strongly on a number of aspects, such as confinement, nozzle-to-plate spacing ( $H/D$ ), nozzle geometry and flow conditions at the nozzle outlet (inflow conditions). This explains the significant amount of work devoted worldwide to this area of research.

The fundamental aspect is the geometry of the problem, primarily with respect to the confinement plate. For a confined impinging jet the flow character and particularly the wall heat transfer change noticeably. Also, as shown in the work by Zukerman and Lior[1], confinement results in lower turbulence level within the axial jet and the potential core becomes, due to less entrainment and spreading of the jet, longer.

The most significant geometrical parameter is  $H/D$  since it is crucial for the flow character within, both, the axial jet and the wall jet.  $H/D$  is often put in relation to the length of the potential core as, for instance, the wall heat transfer, i.e.  $Nu$ , experiences (on average) two maximums if the impingement wall is located within the potential core.

Furthermore, as shown by Cornaro et al. [2] (1999), for  $H/D$  less than two, no discrete vertical structures are formed within the jet shear-layer. Instead the shedding of vortices occurs within the wall jet. For  $H/D = 3$  large scale vortices, shed within the axial jet, are convected downstream. For  $H/D = 4$ , i.e. close to the length of the potential core, the shed vortices are, owing to breakdown and transition to turbulence, not as distinct within the wall jet as for  $H/D = 3$ . Of course, as stated above, this specific behavior is coupled to the considered initial conditions.

As shown by Tu & Wood [3] (1996) the wall pressure distribution was close to Gaussian and remained of similar shape as  $H/D$  was increased from 1 to 12 ( $Re = 11000$ ). The dimensionless stagnation pressure ( $Cp_{stag}$ ) remained on a constant level for  $H/D$  approximately less than 6. For larger  $H/D$ ,  $Cp_{stag}$  decreased proportional to  $(H/D) - 1$ . In the work by Tu & Wood[3] (1996) the measured wall shear stress was compared to the Hiemenz solution (shear increases linearly with the distance from the stagnation point). The slope of  $C_f$  at the stagnation point was considerably steeper for the theoretical relation.

By division of the flow field into four separate regions the magnitude and peak location of the shear stress was derived. A great number of studies are aimed at determining the turbulent characteristics of the impinging jet. This is relevant not only with respect to the physical aspects but also with respect to assessment of turbulence models and numerical schemes. From a steady point of view (RANS approach) turbulent kinetic energy,  $k$ , is produced in the shear-layer of the axial jet, owing to the strong radial gradient of the axial velocity.

The high level of  $k$  results in turbulent diffusion and thus increased jet spreading. If  $H/D$  is large enough also the centre region of the axial jet becomes turbulent. If not, the flow character within the stagnation region resembles that of the potential core.

After deflection the flow develops into a wall jet involving one dominant mean flow gradient that resumes the intense production of turbulence. Two wall parallel regions of production can be identified, one in the outer and one in the inner part of the wall jet. Due to diffusion in the direction of the wall-normal gradient of  $k$  the two shear-layers merge and a turbulent wall jet forms. In the near-wall region production is mainly balanced by viscous dissipation.

The initial region of the impinging jet is called the free jet, for large nozzle to plate spacing the free jet is a characteristic behavior. It can be defined as the jet entering on a large container contains quiescent fluid. The radial velocity decreases continually in the stream wise direction. The region of flow field which is not affected by the growing annular shear layer is called potential core. The flow in potential core is irrotational. As the radial distance goes on increasing, the shear layer instability and roll up starts. The disturbance increases exponentially in the downstream direction.

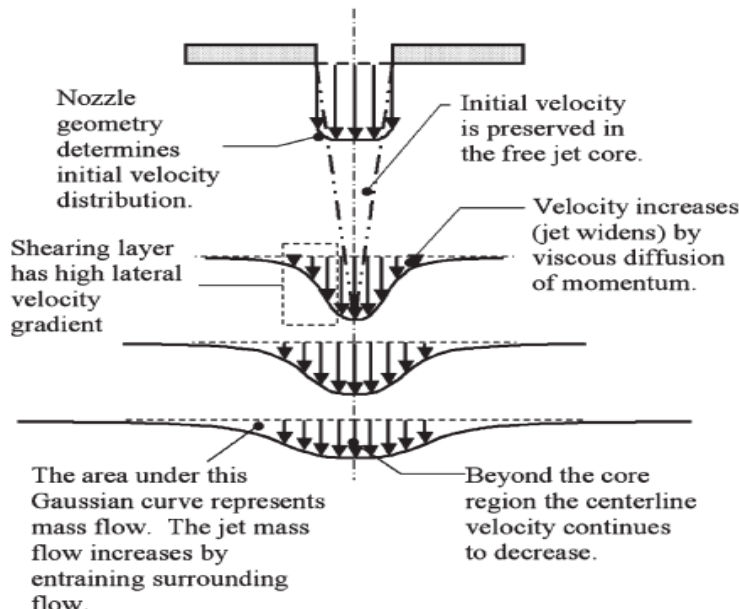


Figure 2: Flow field of a free submerged jet [1]

Figure 2 describes the velocity distribution and potential core region. Beyond the core region the velocity is continually decreases. At approximately 4 diameter downstream of the free jet is fully developed and potential core is no longer present. For an axi-symmetric fully developed free jet, the width of mean axial velocity field determined by the half width.

The self-preserving region of the jet the flow is not influenced by the nozzle exit conditions. At which distance from the nozzle the jet reaches this state is not clear as the results differ significantly within the literature. Some suggest the distance to be around 8D and some up to 70D. The influence from nozzle conditions on jet dynamics and jet self-preservation was studied. They concluded that if there exists an asymptotic jet state, independent of the nozzle conditions, it occurs at distances far larger than 20D.

### **The Stagnation Region**

As the flow approaches the wall, it losses the axial velocity and thus the region labeled as stagnation region. It is shown in figure 2. There the flow builds up on and above the wall. The non-uniform turning flow experiences higher static pressure on and above the wall. The non-uniform turning flow experience high normal and shear stress in the deceleration region. The resulting flow pattern stretches vortices in the flow and increases the turbulences. The stagnation region typically extends 1.2 nozzles diameter for round jet.

### ***The Wall Jet Region***

After turning, the flow enters a wall region where the flow moves latterly outward parallel to the wall. The wall has a minimum thickness within 0.75-3 diameters from the jet axis, and then continually thickness moving thickness further away from the jet axis. This thickness may be measured by the height at which wall parallel flow speed drops to some fraction (5%) of the maximum speed in the wall jet at that radial position. The boundary layer within the wall jet begins in the stagnation region, where it has a typical thickness of no more than 1% of the jet diameter. The wall has a shearing layer which influenced by velocity gradient with respect to stationary fluid at the wall. As the wall jet progresses, it entrain the flow and grows. Due to conversion of momentum, the core of the wall jet may accelerate after the flow turns and as the boundary layer develops.

Sastry et.al. [5], conducted experimental and computational studies on a flat plate to investigate flow characteristics with an array of three rectangular air jets impinging on its top surface. Pressure distribution on the impingement surface and flow visualization experiments with oil lamp black technique were carried out to qualitatively corroborate the computational flow structure with visualized patterns. Computations were carried out by shear stress transport (SST)  $k-\omega$  turbulence model. The jet-to-plate spacing (H) to hydraulic diameter of slot (D) ratio (H/D) was varied from 0.5 to 4.0 and jet Reynolds number (Re) was varied from 5282 to 8450. The computationally obtained flow structure revealed the complex interaction of the wall jets. Primary pressure peaks were observed at the stagnation point and the secondary peaks were noticed at the interaction points of the wall jet. Position of the secondary peaks depends upon H/D and was independent of Reynolds number.

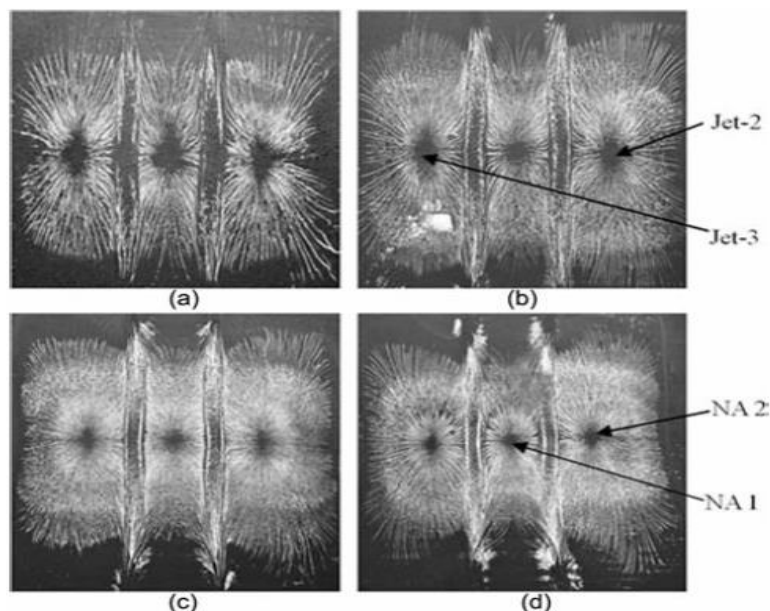


**Figure 3: Experimental flow path lines on the impingement surface for H/D = 2 for Reynolds number (Re) (a) 5282, (b) 6340, (c) 7395 and (d) 8450 [5,6]**

Figure 3 (a), (b), (c), (d) show the surface oil streak lines for H/D=2, at varying Reynolds number of 5282, 6340, 7395, and 8450, respectively. It was observed that the flow behavior remains almost same for all the Reynolds number cases. Overall, the flow structure was independent of Reynolds number.

Sastry et al. [6], carried out computational and experimental studies on a flat plate with an array of five rectangular air jets impinging on its top surface. The array jet consists of a central jet surrounded by four neighboring perimeter jets. Computations were carried out by Shear Stress Transport (SST)  $\kappa-\omega$  turbulence model. The jet-to-plate spacing (H) to hydraulic diameter of slot (D) ratio was varied from 0.5 to 4 and jet Reynolds number was varied from 5282 to 8450. The computationally obtained flow structure revealed the complex interaction of the wall jets. Primary pressure peaks were observed at the stagnation point and the secondary peaks were noticed at the interaction points of the wall jets. Position of the secondary peaks depended upon H/D and was independent of Reynolds number, whereas the size of the peak depended upon both H/D and Reynolds number.

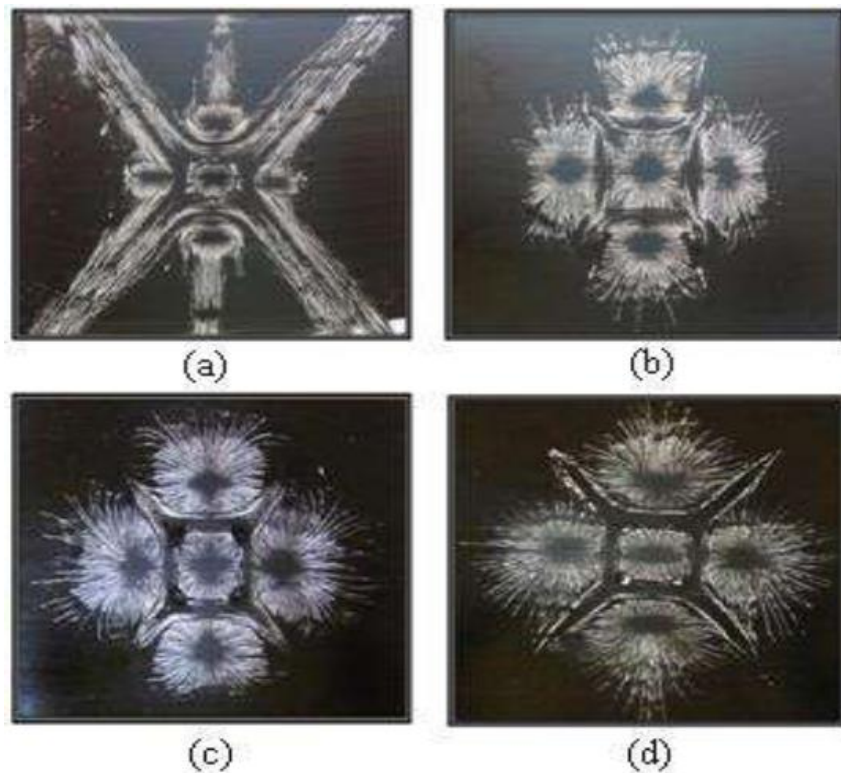


**Figure.4:** Flow structure visualized as traces of oil lamp black on impingement plate, for  $Re = 6340$  (a)  $H/D=0.5$ , (b)  $H/D=1$ , (c)  $H/D=2$ , (d)  $H/d=4$  [5,6]

Figure.4 shows the flow structure visualized as traces of oil lamp black on impingement surface. The shape of the dividing stagnation line was like a square around the central jet with protruding curves separating parameter jets. Position of the secondary peaks moved away from center jets with decrease in  $H/D$ .

Prasad et al. [7] conducted computational and experimental investigations on a flat plate and reported with constant heat flux imposed on bottom surface and five circular jets impinge on a top surface. The five circular jets consists of a central jet surrounded by four neighbouring perimeter jets .Lampblack flow visualization technique and computation using shear stress transformation ( $K-\omega$ ) turbulent model and employed to describe the complex interaction of the wall jets and the associated flow structure. It was observed that the flow topology is practical independent of Reynolds number with in the investigation range but is significantly attend with the spacing between jet orifice and target surface. Primary pressure peaks were observed at the stagnation point and the secondary peaks were noticed at the interaction points of wall jets.

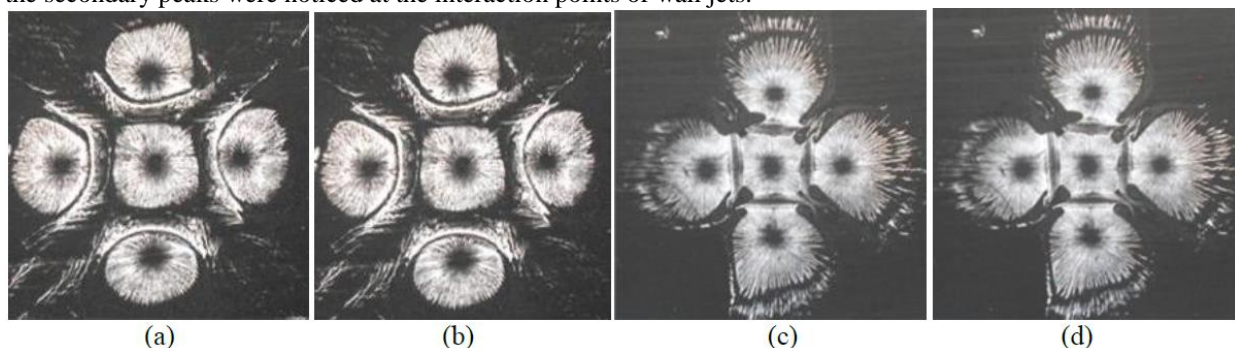


**Figure.5:** Flow structure visualized as traces of oil lamp black on impingement plate, for  $Re = 9075$ , (a)  $H/D=0.5$ , (b)  $H/D=1$ , (c)  $H/D=2$ , (d)  $H/d=4$  [5,6]

Figure.5 shows the visualization of flow structure for  $Re = 9075$ , and  $H/D = 0.5, 1, 2, 4$ . It was seen that the wall jets separate from each other in the impingement plane by the dividing stagnation line.

## II. RESEARCH METHODOLOGY

### Experimental Procedure

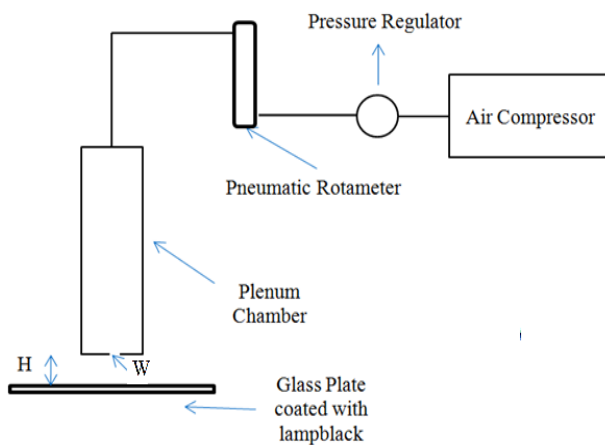


*Figure.6: Schematic layout of experimental Setup*

Figure 1. shows the schematic layout of experimental setup consists of an air supply system including air compressor with compressed air storage tank, pressure regulator, calibrated pneumatic rotameter, single slot orifice, and an impingement surface. The air passes through the dry filter to remove moisture content in the compressed air. Then air passes through the high precision pressure regulator to adjust pressure to the desired value. Then the pressurized air supplied into the plenum chamber containing a mesh screen to reduce the flow fluctuations at the outlet. Air jet for the experiment is obtained by using different orifices at the exit. When the pressurized air goes through the slot hole of width  $w$  and ejects as the rectangular slot jet at the outlet and impinges on the target surface. The air mass flow rate, temperature and pressure were measured directly from gas flow meter, T type thermocouples and pressure gauge respectively.

#### **Flow visualization on the target plate:**

Visualization is an important technique to understand the flow field and mechanism of slot jet flow on the target surface after impinging. The mixture of Lampblack and kerosene is mixed properly. Then the target plate is coated with a mixture of Lampblack and kerosene (thinner) ensuring uniform distribution of mixture on the plate. The Lampblack coated mixture is subjected to impingement under plenum chamber fitted with a orifice of 65mm length having a slot width of 3mm. The air coming from the compressor storage tank is controlled using a Pneumatic Rotameter and is useful for maintaining a constant flow rate. The flow rate is increased till the required flow rate is achieved using a Pneumatic Rotameter. Then the prepared target plate is kept about 15 minutes for impinging and the impingement pattern is obtained. In order to obtain photograph of impingement pattern lampblack visualization photo setup is used. The photograph of impingement pattern is taken using a 13MP camera. The experiment is repeated till the clear photographs of impingement pattern are obtained. For each reading five trials were conducted in order to ensure repeatability of results obtained from the experiments. In all cases, the readings obtained are dimensionally and visually similar. In order to avoid cluster of repeated data and results in report, only one trial out of five is presented. The whole procedure is repeated for different values of flow rates (in) (20 LPM, 30 LPM, 40 LPM, 50 LPM). The different flow patterns are obtained by varying the orifice to plate distance ( $H$ ) by lead screw mechanism. Then the whole procedure is repeated for 5mm slot ( $w$ ) orifice by varying the flow rate and nozzle to plate distance.

#### **Computational Procedure**

The Present Experiment is simulated computationally in ANSYS 14.5, ANSYS Inc. is an international company provides wide range of simulation tool. Since the problem deals with the purely fluid flow and heat transfer, the CFD package of ANSYS which include modeling meshing and a solver is used for computation purpose.

#### **Geometry**

It is the place where the problem was modeled dimensionally. The model prepared as exactly as experimental setup. The dimensions are taken from the experimental setup.

#### **Single slot jet trials:**

Details of Target plate 200 mmx200 mm flat plate.

Slot nozzle width is 3mm and 5 mm

Nozzle to plate distance 9mm (12 mm, 15 mm, 18 mm, 21mm, 24 mm) for 3 mm slot nozzle.

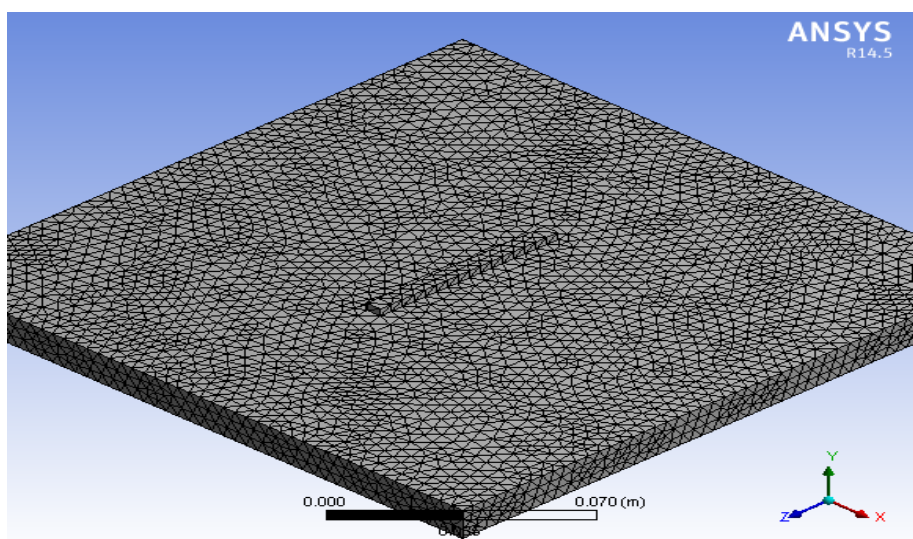
Nozzle to plate distance 10mm (15 mm, 20 mm, 25 mm) for 5 mm slot nozzle.

Jet Height to width ratio (H/w)= 3,4,5,6,7and 8 for 3mm slot nozzle.

Jet Height to width ratio (H/w)= 2,3,4,5 and 6 for 5mm slot nozzle.

#### **Meshing:**

CFD is a technique which solves Navier Stokes equations on the domain in accordance with the boundary condition to give approximate solutions of the fluid flow. Analytical solution of partial differential equations involves closed form of expression which gives the variation of the dependent variables continually throughout the domain. Numerical solution can give in order to solve Navier Stokes equations numerically grid or mesh should be generated on the domain. All the methods in CFD utilize some form of discretization, Here Ansys Fluent solves Navier Stokes equations on each Finite Volume Element. Figure.7 shows the meshed part of the geometric model, it includes polyhedral mesh. The reason for using polyhedral mesh is that it helps in achieving convergence at a faster rate. Mesh sensitivity study is carried out to obtain accurate results.



**Figures.7: Meshed geometries**

Mesh is imported to the ansys fluent solver where the Navier-Stokes equations are solved on the grid points with proper boundary conditions. The boundary conditions are:

For inlet boundary condition: It is given velocity inlet as a Mass flow inlet 20 LPM, 30 LPM, 40 LPM and 50 LPM, Pressure on pressure outlet 0 kPa (Gauge pressure)

#### **Solver settings:**

1. General to be set for pressure based solver.
2. For Models viscous model is set to turbulent model as  $k-\omega$  SST model.
3. For Materials set to be keep Fluid-air and Solid-Aluminium.
4. Boundary conditions: Inlet to be set as a mass flow inlet in kg/s, and turbulence specification method is set to intensity and hydraulic diameter. Give the hydraulic diameter as a 5mm and turbulent intensity as 5%.
5. Solution Method to be Set for Coupled method and on the pseudo transient.
6. Initialization should be done with standard initialization, and run the calculation with giving 1000 iteration. If the solution has not converged in 1000 iteration, but is moving towards convergence, then give 1000 iterations more.

In  $k-\omega$  models, the transport equation for the turbulent dissipation rate,  $\epsilon$ , is replaced with an equation for the specific dissipation rate,  $\omega$ . The turbulent kinetic energy transport equation is still solved. It give much better performance than  $k-\epsilon$  models for boundary layer flows. For separation, transition, and impingement,  $k-\omega$  models are more accurate than  $k-\epsilon$  models. The SST model is a hybrid two-equation model that combines the advantages of both  $k-\epsilon$  and  $k-\omega$  models. It functioned like  $k-\omega$  act near to the wall and  $k-\epsilon$  near the free stream. Since there is no species interaction pressure based solvers is used. Velocity field is obtained from the momentum equation. Mass conservation (continuity) is achieved by solving a pressure correction equation. Pressure-Velocity coupling algorithms are derived by reformatting the continuity equation.

The pressure equation is derived in such a way that the velocity field, corrected by the pressure, satisfies continuity and energy equation. Energy equation (where appropriate) is solved sequentially additional scalar equations are also solved in a segregated (sequential) fashion. Couple model give faster convergence due to coupling of pressure and velocity. The solver must perform enough iteration to reach a converged solution. All equation must be obeyed in the cell within a specified tolerance (Residual). In the energy equation it must range to  $10^{-6}$  and all momentum components must be within the range of  $10^{-6}$  treated as converged solution. The repeated experimental trials were conducted to visualize fluid pathlines and flow field and validated with computational results.

### III. RESULTS AND DISCUSSION

Figure.8 explains the nomenclature used in pictures throughout the results and discussion for a slot jet of 3mm. It explains the visual difference between three regions of topography of flow pattern obtained when a single slot jet (width 3mm) of air impinges on a flat plate, kept perpendicular to the direction of flow of air. The main regions which are identified are stagnation region, maximum shear region, and die out region. To gain insight into how flow rate of air jet affects the topography of flow pattern on impinging plane, from figure.9 (a,b,c,d) results are shown for varying flow rate of jet of air from 20 LPM to 50 LPM. After experimental results, computational fluid dynamics results obtained from Ansys 14.5 based fluent solver is presented from figure.10 and comparison is presented between both of them. Validation between experimental and computational fluid dynamics results from fluent is shown by measuring length of stagnation zone and width of maximum shear zone in both experimental results as well as CFD results. To show accuracy of mesh, number of nodes, number of elements is mentioned below the results. Also, length of stagnation zone and width of maximum shear zone in both experimental and CFD case is displayed below the figure for better understanding. Figure.8 shows the different regions, which are obtained on the target plate, when a single slot jet of slot width 3mm impinges on it. From the figure it can be seen that the impingement pattern is very close to elliptical shape. When a jet of air coming from the compressor impinges on the target plate coated with lampblack mixture 3 regions are observed.

- Stagnation region
- Maximum Shear region
- Die out region

The inner most regions is called as stagnation region and it is the area of plate which is subjected to maximum pressure and lowest shear force. The cause of stagnation region is that when jet of air impinges on the target plate, instead of moving outward, creating a shearing effect on wall, they first bounce and then move outward in maximum shear region. From the figure.8 it can be seen that the width of stagnation region is almost equal to the width of slot jet used to conduct the experiment, which is 3 mm. Also the length of stagnation region is approximately equal to the length of slot nozzle used to conduct the experiment, which is equal to 65 mm.

The region outside the stagnation region is called as Maximum Shear Region and in this region maximum erosion of surface takes place, on account of high shear effects. The width of stagnation region varies with respect to both flow rates as well as H/w ratio. Higher the flow rates higher will be the shear region, lower the flow rate lower the width of maximum shear region.

After sufficient time of impingement the flow enters a wall region where the flow moves latterly outward parallel to the wall and it is the outermost region in which effect of jet can be seen and it is called as Die Out Region and by the time jet of air reaches this region, it had lost most of its energy because of friction with the surface. Due to insufficient energy, it is not able to overcome the friction between the surface and air and thus, the air jet separates from the wall.

Experimental results for lampblack visualization on target plate for a slot jet of (3mm x 65 mm).

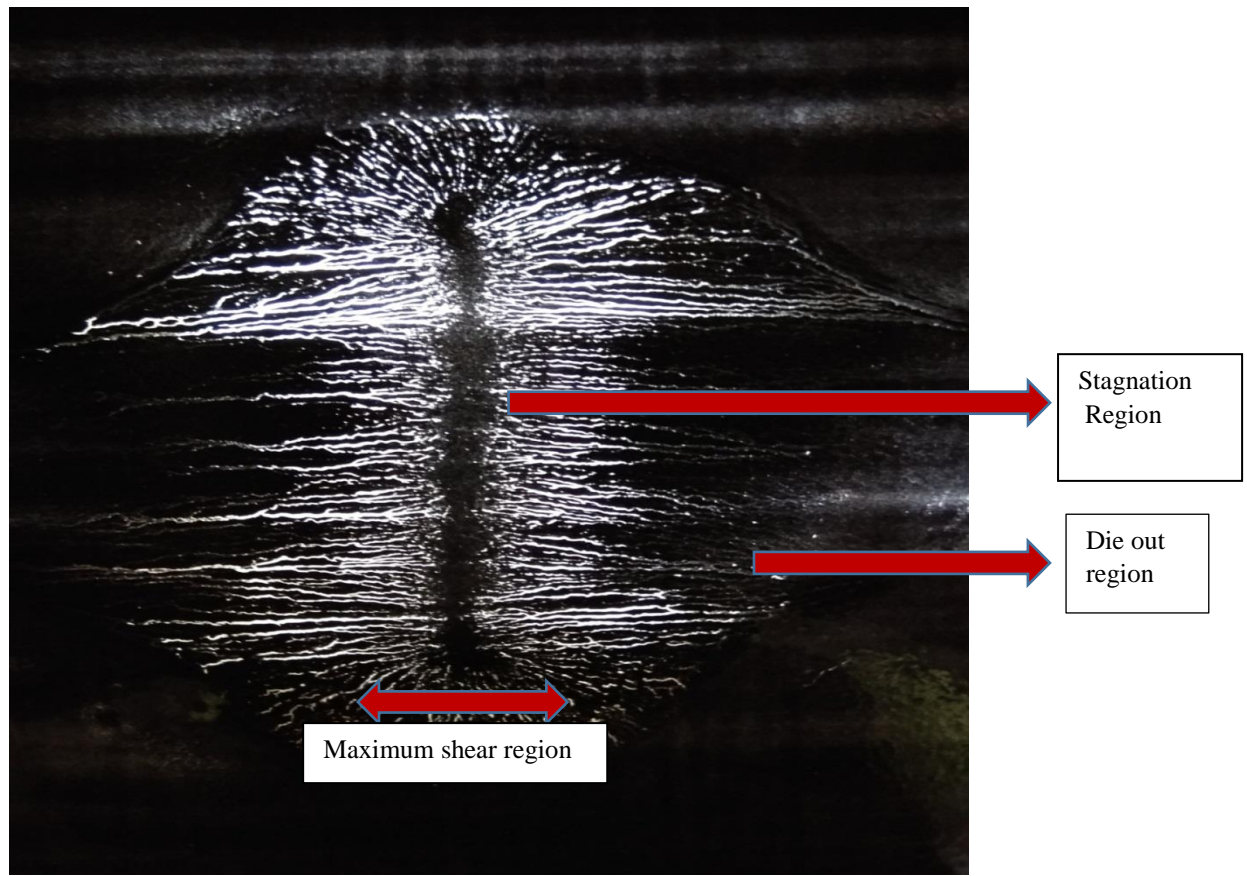
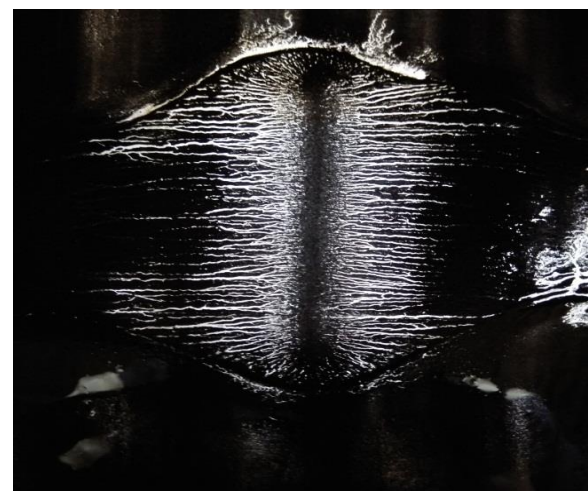


**Figure.8: Nomenclature of flow structure visualized for typical case study of rectangular slot (width 3mm x length 65 mm) and 30 LPM flow rate of air for H/w=7.**

Figure.9 shows the lampblack visualization for single slot air jet impingement from nozzle of slot width 3 mm and with a nozzle to plate distance of 9 mm. From the figures it is observed that the impingement pattern is very close to elliptical in nature. It is very important to note that the H/w ratio is kept at 3 for the above cases. Figure.9 (a) to (d) shows how the jet moves in all direction after impinging on the flat target plate. With increase in Reynolds number i,e mass flow rate the area of maximum shear region and die out region also increases. The length of stagnation region is almost same as the length of nozzle slot used to conduct the experiment and the width of the stagnation region is almost same as the width of nozzle slot used here, which is 3mm. The width of maximum shear zone increases with increase in mass flow rate.



a) 20 LPM



b) 30 LPM



c) 40 LPM



d) 50 LPM

**Figure.9:** Lampblack visualization on target plate for single slot jet of width ( $w$ ) 3mm and height ( $H$ ) 9 mm and at different mass flow rate of air jet

Computational results for lampblack visualization on target plate for slot jet of 3 mm.

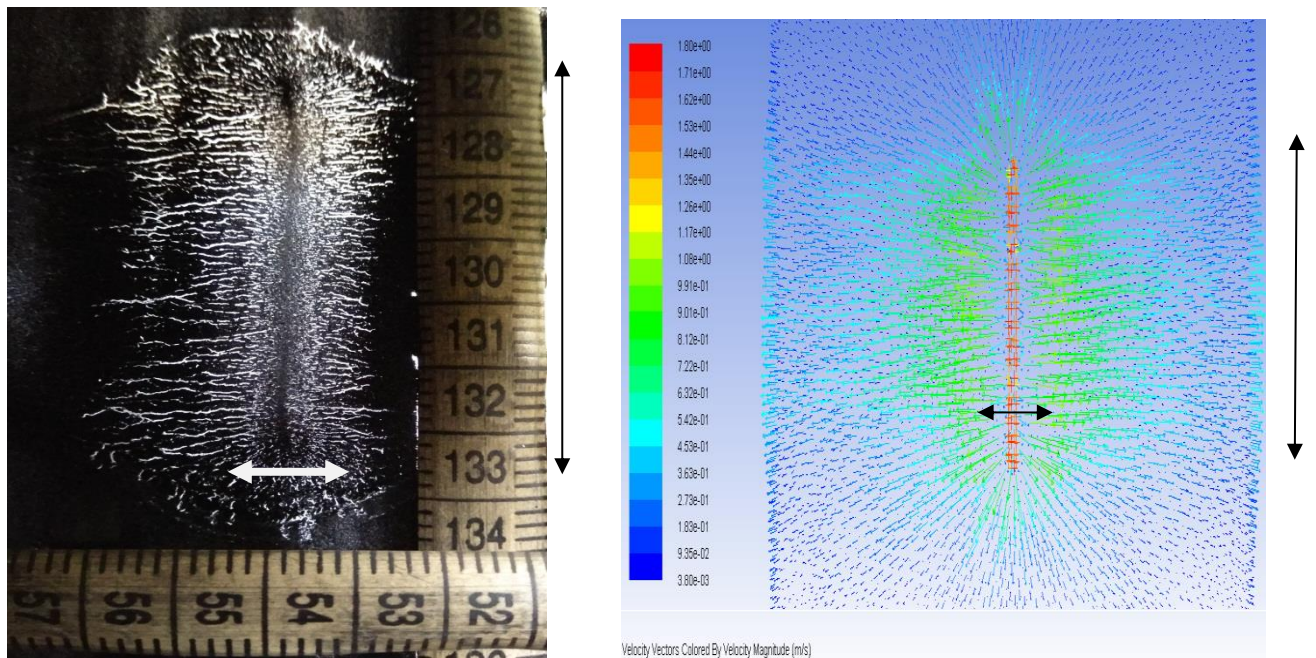


**Figure.10:** comparison of experimental and computed flow path lines for slot jet width ( $w$ )3 mm and height ( $H$ )9 mm for mass flow rate of air 20 LPM.

65mm  $\longleftrightarrow$  Stagnation zone length  $\longrightarrow$  54mm  
 15mm  $\longleftrightarrow$  Maximum shear zone width  $\longrightarrow$  10mm

Mesh quality: Nodes-13278, Elements-58476

Figure.10 shows a comparison between experimental results obtained in lampblack visualization and Computational Fluid Dynamics (CFD) results obtained on Ansys14.5 software for single slot jet impingement on flat surface for a nozzle of slot width 3 mm, nozzle to plate distance of 9 mm and flow rate of air equal to 20 LPM. It can be easily seen from the figure that computed results and experimentally visualized flow structures qualitatively agree with each other. Results were compared by measuring the length of stagnation zone and width of maximum shear zone. The measured length of stagnation zone in experiment is 65 mm and in CFD is 54 mm and hence the difference is 11 mm. The width of maximum shear zone in experiment is 15mm and in CFD is 10 mm and hence the difference is 5 mm. It has been identified preferred method to measure width of stagnation zone and maximum shear zone. These zones influence in transfer of heat energy and mass in industrial applications. From jet impingement heat transfer literature it is observed that there is high rate of heat energy dissipation is observed at stagnation zone. Secondary peaks of heat transfer are also observed besides stagnation zone in case multi slot jet heat transfer study because of the spent flow after the impingement influences in creating turbulence in surrounding fluid. From current research study it is revealed that maximum shear zone width is influences in selection of neighboring jets besides the primary jet. For case considered for study from figure.10, neighboring jets should be selected 15 mm away from the stagnation zone there by secondary heat transfer peaks can be achieved so that it enhances heat transfer in multi jet impingement cooling. This study gives clear idea how to choose multi slot jets side by side at correct distance from central stagnation zone. It also helps in avoiding abrasion of the surface particulates for mass transfer applications. Selection of efficient configuration of multi slot impingement arrangements offers efficient use of the fluid and for maintaining necessary cooling rate.

#### IV. CONCLUSIONS

An experimental work has been carried out for a single slot jet impingement on a flat plate to study the effect of H/W ratio, flow rates and how the jet moves in all direction once it impinges on the plate by using lampblack visualization technique for two different slots of 3mm and 5mm. Experimentation is done to study the flow pattern topography on the flat target plate, with varying the flow rate from 20 LPM to 50 LPM by varying the nozzle to plate distance from 9 mm to 24 mm (H/w ratio varies from 3 to 8) for slot jet of 3mm and varying the nozzle to plate distance from 10 mm to 30 mm (H/w ratio varies from 2 to 6) for slot jet of 5mm.

Computational work also performed using Ansys14.5 software and comparison is made with experimental results. Based on the experimental and computational work following conclusions have been drawn.

1. Formation of 3 distinct regions
  - Stagnation region
  - Maximum Shear region
  - Die out region
2. With increase in Reynolds number i.e, mass flow rate, areas of above three regions increases.
3. The width of stagnation region formed is approximately equal to the width of slot jet used to conduct the experiment and also the length of stagnation region is approximately equal to the length of nozzle slot used for study.
4. With increase of H/w ratio both stagnation zone and maximum shear zone decreases slightly due to low pressure impingement of air on the target plate.
5. CFD results obtained from ANSYS 14.5, FLUENT are helpful in approximately predicting the width of maximum shear zone and length of stagnation zone numerically.
6. The numerical analysis is validated with experimental work by measuring the length of stagnation region and width of maximum shear zone in both experimental results as well as computational fluid dynamics (CFD) results obtained with the help of Ansys software and fluent workbench, and it is observed that the experimental results match with CFD results with error less than 15%.
7. The wall jet separates from the plate wall at the end of die out region due to boundary layer separation on account of lack of energy to overcome friction between plate wall and air.

8. Selection of multi slot jet configuration can be decided by understanding the formation of maximum shear region there by abrasion of the surface can be minimized by maintain necessary cooling rate.

## NOMENCLATURE

H - Nozzle to target plate height in mm.  
 w - Width of slot jet.  
 H/w - Nozzle height to width ratio.

## V. REFERENCES

1. N. Zuckerman and N. Lior, Jet Impingement Heat Transfer: Physics, Correlations, and Numerical Modelling, Advances In Heat Transfer Vol.39, (2006) 565-631.
2. C. Cornaro, A.S. Fleischer, R.J. Goldstein, Flow visualization of a round jet impinging on cylindrical surfaces, Experimental Thermal and Fluid Science 20 (1999) 66-78.
3. C. V. Tu, D. H. Wood, Wall Pressure and Shear Stress Measurements Beneath an Impinging Jet, Experimental Thermal and Fluid Science 1996: 13:364-373.
4. V Katti and SV Prabhu Heat transfer enhancement on flat surface with axisymmetric detached ribs by normal impingement of circular jets International Journal of Heat and Fluid Flow 29(2008)1270-1284.
5. M.R.CH. Sastry, BVSSS Prasad and AVSSKS Gupta (2015), "Experimental and Computational study of fluid flow on a plate with three rectangular impinging slot jets", International Journal of Engineering and Material Science, Vol.22, pp.631-640.
6. M.R.CH. Sastry, BVSSS Prasad and AVSSKS Gupta (2014), "Study of fluid flow on a flat plate with multiple rectangular impinging slot jets", International Journal of Engineering Trends and Technology, Vol. 13, No.2.
7. K. Durga Prasad, K.Ravikumar,M.R.CH Shastry Fluid flow and Heat transfer analysis of turbulent multiple circular jet impinging on a flat plate. IJERT 9 (2012).
8. A.S.Fleischer<sup>a,1</sup>, K. Kramer <sup>b</sup>, R.J. Goldstein <sup>c,\*</sup> , Dynamics of the vortex structure of a jet impinging on a convex surface , Experimental Thermal and Fluid Science 24 (2001) 169-175
9. Mansoo Choi, Han SeoungYoo, Geunyoung Yang, Joon Sik Lee, Dong KeeSohn<sup>a,b</sup>,Measurements of impinging jet flow and heat transfer on a semi-circular concave surface, Int J Heat and mass transfer 43(2000) 1811-1822
10. Gardon R and Akfart.J.C(1965) The role of turbulence in determining the heat transfer characteristics of impinging jets International Journal .Heat and Mass transfer 8,1261-1272.
11. Gaunter J.W Livingood.JNB and Hrycak.P(1970) Survey of literature on flow characteristics of singe turbulent jet impinging on flat surfaces.NASA TN D-5652 NTIS N70 1896
12. Haydar Eren, Nevin Celik, Bulent Yesilata, Nonlinear flow and Heat transfer dynamics of a slot jet impinging on a slightly curved concave surface, Int. Communications in Heat and Mass Transfer 33(2006) 364-371.
13. Geunyoung Yang, Mansoo Choi, JoonSik Lee, An experimental study jet impingement cooling on concave surface: effects of nozzle configuration and curvature, Int. Journal of Heat and Mass Transfer 42(1999) 2199-2209
14. Raymond E Chupp and Haeold Helmst Evaluation of internal heat transfer coefficient for impingement cooled turbine airfoils J.AircraftVol 6,No 3 1969.
15. N.Kayansayan, S. Kucuka, Impingement cooling of a semi-cylindrical concave channel by confined slot-air-jet, Experimental Thermal and Fluid science 25(2001) 383-396.
16. Neil Zuckerman, and Noam Lior, Radial Slot Jet Impingement Flow and Heat Transfer on a Cylindrical Target, Journal of Thermodynamics and Heat Transfer Vol.21, No.3, July-September 2007.
17. A. M. Tahsini, and S. Tadayon Mousavi, Laminar Impinging Jet Heat Transfer for Curved Plates, World Academy of Science, Engineering and Technology, Vol:6 2012-12-26.
18. Satheesha .V, B.K Muralidhara, C.K. Umesh, "Study on heat transfer during rectangular slot air jet impingement on curved surfaces", International Journal of Theoretical and Applied Mechanics, Research India Publication, ISSN 0973-6085, Volume-12, Number-2, 2017, pp 209-226.
19. Satheesha .V, B.K. Muralidhara, C.K. Umesh, "Experimental and computational analysis of Heat transfer, fluid flow and pressure distribution of multi-jet impingement on concave surfaces", Proceedings of International Conference on Advances in Mechanical Engineering Sciences, ISBN: 978-81-932966-3-9 at PES College of Engineering, Mandy on 21<sup>st</sup>-22<sup>nd</sup> April-2017.
20. Satheesha .V , B. K Muralidhara, C.K. Umesh, "Study on heat transfer during rectangular slot air jet impingement on curved surfaces", 24<sup>th</sup> National and 2<sup>nd</sup> International ISHMT-ASTFE Heat and Mass Transfer Conference (IHMTC-2017), December 27-30, 2017, BITS Pilani, Hyderabad Campus.